京都大学防災研究所年報 第41号 B-1 平成10年4月
Annuals of Disas. Prev. Res. Inst., Kyoto Univ., No. 41 B-1, 1998

Simulation of Activity of Large Earthquakes in and Around Southwest Japan on the Basis of Back-Slip Model

Manabu HASHIMOTO

Synopsis

Activity of large earthquakes in southwest Japan is simulated with a model incorporating mechanical interactions between inter- and intraplate faults. In this model, stress on each fault accumulate by constant back-slip derived from inversion of geodetic data and, when cumulative stress of a fault is larger than assumed thresholds, that fault slips forward and stress is redistributed.

The results of simulations show that interaction causes complex patterns (e.g. cascade, migration etc.). Recurrence intervals of events at some faults fluctuate around an average. Other group of faults, especially around the Kii peninsula, have more than two discrete recurrence intervals. Simulations indicate that small errors in parameters may produce large difference in seismicity after hundreds of years.

Keywords: Simulated Seismicity; Fault interaction; Coulomb Failure Function; Recurrence; Back-slip model

1. Introduction

Recently the Earthquake Research Committee, the Headquarters of Earthquake Research Promotion of the Japanese government, released evaluations of long-term activity of two inland active fault systems. These evaluations are based on the history of activity of fault deduced from geological studies, especially excavation, and characteristic earthquake model (Schwarz and Coppersmith, 1984). These evaluations can only imply the possibilities of occurrence of large events on the specified fault system for several hundred years including the present. It is the best considering the accuracy of dating of previous events identified in the excavation studies. Therefore development of a forecasting method, which can incorporate new accurate data obtained by seismology, geodesy and so on, are expected.

The characteristic earthquake model, adopted in the above evaluations, assumes that slip events with same amount and spacial extent recur periodically at the specified fault. However this model ignores other faults in the vicinity of the fault under consideration. Recent study on the coseismic stress changes show faulting of one fault affects seismicity in its surrounding area (e.g. Hudnut et al.,,1989; Harris and Simpson,1992; Jaume and Sykes, 1992; King et al,1994; Hashimoto, 1995,1997). Therefore it is worthwhile to quantitatively evaluate the effect of faulting in the surrounding region on the recurrence behavior of slip at specified fault and examine to what extent the assumption of characteristic earthquake can be valid.

Theoretical model to simulate seismicity has been studied mainly with block and slider model in which the block on frictional surface is being loaded through a spring connected to the block. Since Burridge and Knopoff (1967) dealt with this model to simulate stick-slip events, this block and slider model has been significantly studied and led Carlson and Langer (1989) and Ito and Matsuzaki (1989) to the idea of self-organized criticality. Huang and Turcotte (1990) and Ruff (1992) also showed complexity of modeled seismicity with two block model connected each other with additional spring. However these models assume regular distribution of blocks and constant stiffness of spring connecting blocks which gives symmetrical interaction between blocks. Actual faults are rather irregularly distributed than blocks in these models, which implies asymmetrical interaction between faults. Rundle (1988a) developed a method to deal with such an interaction between real fault systems. Rundle (1988b) applied his method to the fault system in southern California. Ward (1996) also

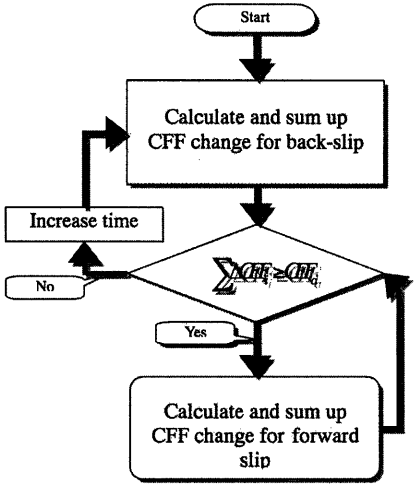

Fig. 1. Flow diagram of calculation

made a similar study incorporating much more details of fault system in southern California than Rundle (1988b). These studies show rather complicated pattern of recurrence of large slip events at a specified fault fault than the characteristic earthquake model. In southern California strike-slip faults such as San Andreas fault are dominant. In southwest Japan, on the other hand, shallow dipping thrusts are dominant along the Nankai trough, but strike-slip faults are usually seen in inland region. Furthermore slip rate of faults along the Nankai trough is larger than that of inland fault by a factor of 10. Thus geometry of fault system is very different between southern California and southwest Japan. It is interesting to see what happens in modeled seismicity for such a different fault system.

Interplate coupling at the Nankai trough is considered to be the main controlling factor of seismicity in inland region of southwest Japan. Hori and Oike (1996) show temporal correlation between large inland events and interplate thrust events. It is controversial what mechanism is responsible for arising such a correlation (Hashimoto, 1998; Pollitz and Sacks, 1997; Hori and Oike, 1998).

The above three issues are to be resolved in order to develop long-term forecasting methods with enough sufficient reliability for the public use. In this paper, I present a simple interacting fault model of southwest Japan and simulate activity of large events to examine their complexity and predictability.

2. Scheme of Simulation

This simulation adopts a kind of time-marching method: i.e. stress state of fault at an arbitrary time are calculated by adding increments due to movements of all faults during given time interval to the stresses at the previous time step. Flow diagram of simulation is shown in Fig.1. In this paper, the time interval for calculation of increment is 1 year.

Mechanical interaction between fault faults are represented as change in Coulomb Failure Function (hereafter ΔCFF) for preferred slip of each fault induced by slip events of other faults in their preferred direction. Δ CFF is evaluated the center of each fault. I assume perfect elastic half space in the calculation of stress and use Okada's (1992) formula. Preferred slip of each fault are reduced by the results of inversion of geodetic data (Hashimoto and Jackson, 1993). The first step of simulation is to calculate this ΔCFF of each fault due to unit slip of all fault and store them as a matrix in memory. I call this matrix as "interaction matrix" tentatively. Be aware that the derivation and definition of interaction matrix is different from Rundle and Kanamori (1987) and Rundle (1988a).

Initial state of faults is given by distributing stresses randomly within the interval of 0 and threshold for rupture. Beginning from this initial state, stresses of all faults change according to their movements. Movements of faults are divided into two categories: back- and forward-slips. Back-slip represents the accumulation process of stress (Savage, 1982; Matsu'ura et al., 1986). On the other hand, forward slip is an earthquake. When accumulated ΔCFF for a fault exceeds its rupture threshold, forward slip occurs and stress is redistributed referring to the interaction matrix and the amount of slip. In this study, I assume forward slip releases all the accumulated stress for the rupturing fault. This assumption implies that fault obeys characteristic earthquake model, without interaction. Otherwise, stress accumulates in proportion to their back-slip rate estimated by inversion of geodetic data. This judgement is done at every time step. If there is a rupturing fault, all the accumulated stress is redistributed and added to the other faults. After adding stress changes to other faults, the judgement of rupture is repeated for all faults till no rupturing faults are found. If there are no rupturing faults, calculation goes to the next time step. The calculation will be continued till the desired time. I calculate stress history for 10,000 years in order to avoid the artificial effect of initial state and see many events at all faults enough to discuss recurrence behavior in this study.

I refer to Hashimoto and Jackson (1993) for the model of fault system of southwest Japan (Fig.2). All faults are assumed to be rectangle with uniform slip. Rectangles in Fig. 2 are projection of dipping fault planes to the surface and thick lines show their

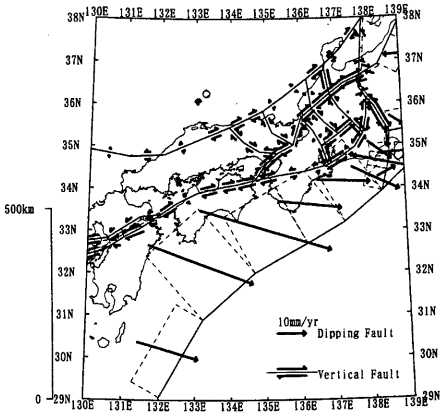

Fig. 2. Block-fault model and back-slip adopted in this study (Hashimoto and Jackson, 1993)

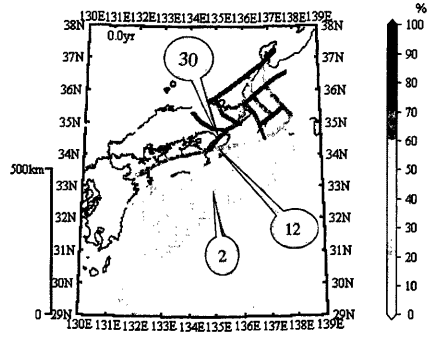

Fig. 3. Initial state of the present simulation. Recurrence pattern of faults with number are discussed later.

upper margins. Strike-slip faults are indicated as thick lines with parallel arrows in opposite directions. Arrows show forward slip derived from inversion. Hashimoto and Jackson (1993) modeled whole Japanese Islands, but I adopted 62 faults from their model due to the limitation of system resource. The parameters of adopted model faults are shown in Table 1. A couple of faults has different slip direction than neighboring faults. Neighboring faults, which have much larger slip rates, decrease Δ CFF of these faults and keep away from rupture. However absolute value of Δ CFF finally exceeds the threshold during simulation, which is unphysical. Since slip rate of these faults is less than estimated errors, I reverse slip direction of these faults to avoid this situation. Initial state is shown in Fig. 3.

Rupture threshold is one of the key parameters, which control the timing of rupture and magnitude of slip. In this study I assume forward slip of each fault be as large as those of observed events at corresponding or similar real faults: 4~6m for interplate boundaries such as the Nankai and Suruga troughs and 2m for inland faults, respectively. According to Tsutsumi and Okada (1995), slip of the latest event at the MTL may be ~ 6m. Therefore I examine the cases with large threshold for MTL and all inland faults.

3. Results

3.1 Complexity of Simulated Seismicity

Fig.4 shows the history of events during 10,000 years. Interplate boundary faults slips very regularly in time. However, recurrence interval of faults off Kii peninsula is much longer (500 ~ 1,000 years) than that of off-Shikoku faults (~ 100 years). This may be attributed to the geometry of faults off Kii peninsula, where significant parts of fault plane is overlapped (Fig.2). Since the mechanical interaction during interseismic period are taken into consideration, these faults tend to decrease their stresses each other.

Activity along the Median Tectonic Line (hereafter MTL) is very complicated. There is a tendency that rupture of faults of MTL occur closely in time. However sometimes rupture propagates from east to west and vice versa. Several epochs include cascade, in which multiple faults rupture at the same time. Fossa Magna also has similar tendency. It is difficult to notify such a tendency for other fault systems, because they are much shorter than MTL and Fossa Magna.

It should be recognized that activity of inland faults is much higher than observed seismicity. Back-slip rates using in this study are derived from geodetic data. It is well known that strain rates deduced by geodetic data are higher than those estimated by geological and seismological studies by a factor of 10. Therefore stress accumulation rates are overestimated for inland fault, especially MTL, in this study.

Fig.5 shows snapshots of events for every 100 years during the period from 2,400 to 3,600 years. Interplate events along the Nankai trough occur every 100 years, but the ruptured faults are not the same at every epoch. It is interesting that rupture extends along MTL from Shikoku to the Kii peninsula in the case for 2,600 ~2,700 years, while faults on the Awaji island and the Rokko fault system ruptures along with the MTL in Shikoku and the fault on the Kii peninsula does not for 3,200 ~ 3,300 years.

Table 1. Parameters of block boundary faults

ID	Name	Lat.	Lon.	L(km)	W(km)	δ (deg)	φ (deg)	Us (m m/yr)	Ud (m m/yr)
0	NT1	33.918	138.369	130.3	172.8	10	232	-14.35 ± 2.78	12.65 ± 2.53
1	NT2	33.202	137.251	114.6	172.8	10	241	-17.86 ± 3.61	13.13 ± 3.77
2	NT3	32.701	136.174	159.1	172.8	10	241	-33.59 ± 3.49	35.55 ± 3.84
3	NT4	32.008	134.686	185.4	230.4	10	228	-18.68 ± 3.53	35.75 ± 3.54
4	NT5	30.899	133.219	233.9	87.7	20	210	-5.39 ± 4.37	23.20 ± 5.84
5	MTL01	35.706	137.975	44.0	20.0	90	3	-2.53 ± 3.85	0.00 ± 0.16
6	MTL02	35.276	137.866	48.8	20.0	90	12	-4.01 ± 3.54	0.01 ± 0.16
7	MTL03	34.968	137.609	41.3	20.0	90	34	4.64 ± 2.75	-0.01 ± 0.16
8	MTL04	34.753	137.233	41.8	20.0	90	55	1.07 ± 1.72	0.00 ± 0.16
9	MTL05	34.549	136.812	44.5	20.0	90	60	7.84 ± 3.33	-0.01 ± 0.16
10	MTL06	34.405	136.136	63.9	20.0	90	75	-1.04 ± 3.62	0.01 ± 0.16
11	MTL07	34.320	135.443	64.2	20.0	90	82	1.82 ± 3.30	0.00 ± 0.16
12	MTL08	34.201	134.702	69.2	20.0	90	79	-5.26 ± 2.57	-0.01 ± 0.16
13	MTL09	34.102	134.182	49.0	20.0	90	77	-6.00 ± 3.28	0.00 ± 0.16
14	MTL10	34.034	133.701	44.9	20.0	90	80	-3.92 ± 3.96	0.00 ± 0.16
15	MTL11	33.895	133.032	63.5	20.0	90	76	-4.85 ± 3.47	-0.01 ± 0.16
16	MTL12	33.645	132.436	61.5	20.0	90	63	-0.68 ± 2.79	-0.01 ± 0.16
17	MTL13	33.389	131.992	49.9	20.0	90	55	-4.89 ± 3.37	-0.01 ± 0.16
18	A1	36.896	136.723	76.3	20.0	90	170	-5.90 ± 3.39	0.00 ± 0.16
19	A2	36.220	136.875	45.3	20.0	90	146	-1.58 ± 4.30	0.00 ± 0.16
20	A3	35.881	137.158	52.3	20.0	90	136	-0.13 ± 4.21	0.00 ± 0.16
21	A4	35.543	137.563	40.4	20.0	90	137	5.61 ± 2.89	0.00 ± 0.16
22	N1	36.579	136.211	78.8	20.0	90	171	0.53 ± 4.96	0.00 ± 0.16
23	N2	35.877	136.344	49.3	20.0	90	137	-1.87 ± 4.01	0.00 ± 0.16
24	N3	35.552	136.718	48.0	20.0	90	131	-2.56 ± 4.29	-0.01 ± 0.16
25	Yr1	35.665	136.041	44.9	20.0	90	138	2.66 ± 4.19	0.00 ± 0.16
26	Yr2	35.364	136.372	46.6	20.0	90	151	-0.60 ± 3.88	0.00 ± 0.16
27	Yr3	34.997	136.623	52.5	20.0	90	161	5.26 ± 3.24	0.01 ± 0.16
28	H	35.025	135.807	74.1	20.0	90	17	-3.18 ± 2.00	-0.01 ± 0.16
29	AT1	34.827	135.354	46.7	20.0	90	62	-3.26 ± 3.75	0.00 ± 0.16
30	AT2	34.573	135.005	42.5	20.0	90	49	-8.32 ± 2.90	0.00 ± 0.16
31	AT3	34.201	134.702	49.7	20.0	90	34	-2.16 ± 2.77	0.00 ± 0.16
32	Ta1	35.827	134.935	61.7	20.0	90	157	-1.80 ± 2.33	-0.01 ± 0.16
33	Ta2	35.317	135.206	63.4	20.0	90	121	-2.04 ± 3.44	0.01 ± 0.16
34	Ys1	35.449	133.959	52.4	20.0	90	137	-2.20 ± 2.40	0.01 ± 0.16
35	Ys2	35.106	134.356	50.9	20.0	90	121	-2.36 ± 3.52	0.00 ± 0.16
36	Ys3	34.871	134.838	47.2	20.0	90	96	2.73 ± 3.43	0.00 ± 0.16
37	As1	36.468	137.299	48.5	20.0	90	67	-8.86 ± 3.73	-0.01 ± 0.16
38	As2	36.220	136.875	46.8	20.0	90	54	-9.69 ± 3.44	0.01 ± 0.16
39	As3	35.877	136.344	61.0	20.0	90	51	-4.52 ± 4.95	0.00 ± 0.16
40	As4	35.665	136.041	36.0	20.0	90	49	-5.33 ± 4.16	0.00 ± 0.16
41	C1	35.271	137.120	50.2	20.0	90	53	6.50 ± 3.93	0.01 ± 0.16
42	C2	34.997	136.623	54.5	20.0	90	56	-3.25 ± 4.01	0.00 ± 0.16
43	CJF4	36.896	136.723	63.0	20.0	90	48	-1.66 ± 3.37	-0.01 ± 0.16
44	SJF1	36.579	136.211	57.5	20.0	90	52	-3.94 ± 4.20	0.00 ± 0.16
45	SJF2	36.143	135.499	79.9	20.0	90	53	-0.60 ± 4.35	0.00 ± 0.16
46	SJF3	35.827	134.935	61.6	20.0	90	55	0.68 ± 4.17	0.00 ± 0.16
47	SJF4	35.637	134.452	48.3	20.0	90	64	-2.70 ± 3.47	-0.01 ± 0.16
48	SJF5	35.449	133.959	49.1	20.0	90	65	-3.46 ± 2.44	0.01 ± 0.16
49	SJF6	35.166	133.114	82.7	20.0	90	68	-3.30 ± 2.78	-0.01 ± 0.16
50	SJF7	34.803	132.078	102.4	20.0	90	67	0.88 ± 2.87	0.01 ± 0.16
51	SJF8	34.760	131.105	88.8	20.0	90	87	1.81 ± 3.56	0.00 ± 0.16

Table 1. (continued)

ID	Name	Lat.	Lon.	L(km)	W(km)	δ (deg)	ϕ (deg)	Us (m m/yr)	Ud (m m/yr)
52	SJF9	34.917	129.946	107.0	20.0	90	99	-0.41 ± 4.12	0.00 ± 0.16
53	FM3	36.366	137.764	30.6	21.3	70	6	-1.10 ± 3.95	9.50 ± 3.53
54	FM4	36.102	137.998	36.0	21.3	70	324	0.66 ± 3.64	5.78 ± 3.70
55	FM5	35.905	138.221	29.6	20.0	90	318	3.56 ± 4.06	0.00 ± 0.16
56	FM6	35.615	138.408	36.3	20.0	90	332	8.61 ± 2.91	0.01 ± 0.16
57	FM7	35.293	138.632	41.2	20.0	90	330	-2.94 ± 2.68	0.00 ± 0.16
58	FM8	35.293	138.632	30.2	31.9	70	185	6.86 ± 4.03	3.32 ± 6.26
59	SrT1	35.021	138.604	33.7	60.0	30	179	6.33 ± 3.16	9.11 ± 3.75
60	SrT2	34.717	138.613	36.1	60.0	30	195	-0.50 ± 3.32	23.53 ± 4.67
61	SrT3	34.402	138.514	55.3	60.0	30	194	3.98 ± 3.63	21.04 ± 5.79

Lat. And Lon. are latitude and longitude of the northeastern edge of fault, respectively. L and W are length and width, respectively. Depth of upper margin of all faults are assumed to be 0. δ and ϕ are dip and strike (clockwise from north), respectively. Us and Ud are strike- and dip-slip components of forward slip rates, respectively, in mm/yr. Left lateral and thrust motion are positive, respectively. Name of faults are referred to Hashimoto and Jackson(1993).

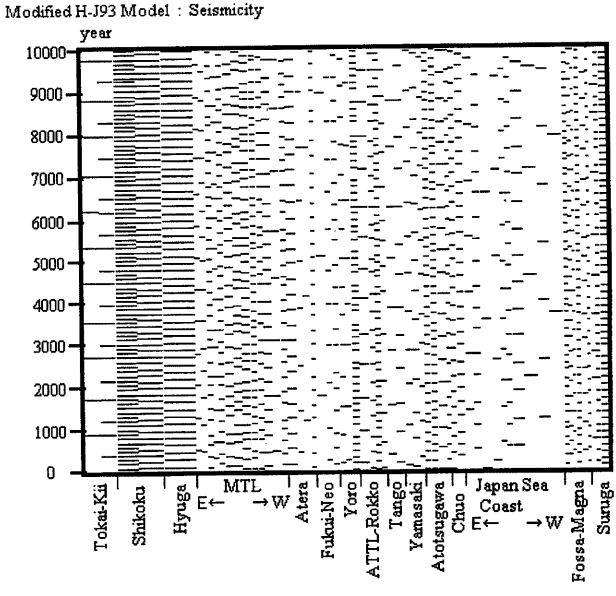

Fig. 4. Time series of events in case with mechanical interaction. Each line indicates event. Its length is proportional to fault length.

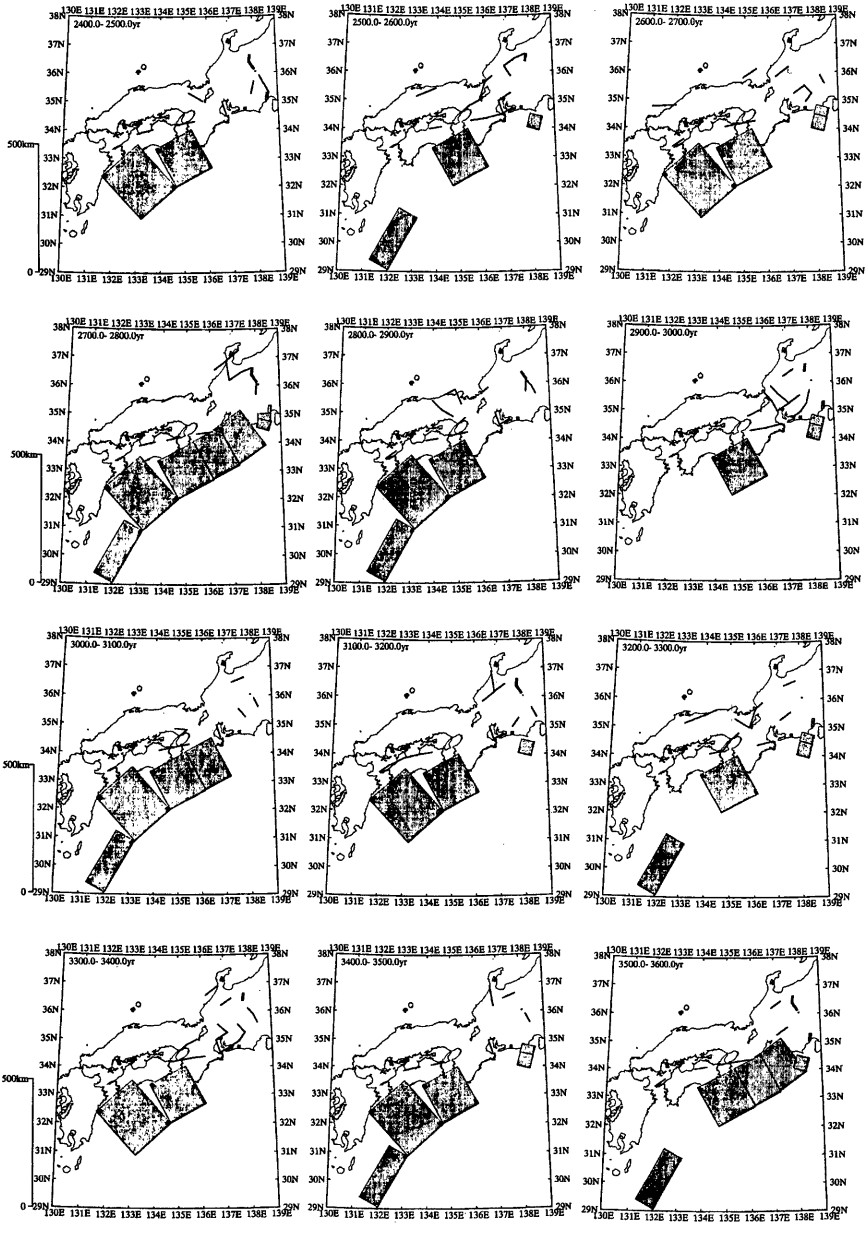

Fig. 5. Snapshots of events every 100 years during the period from 2400 to 3600. Black rectangles and lines show ruptured faults.

(a)

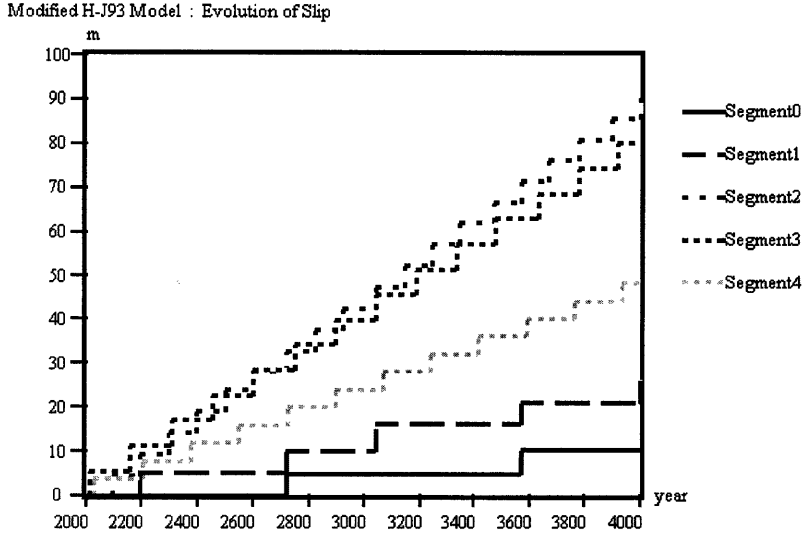

(b)

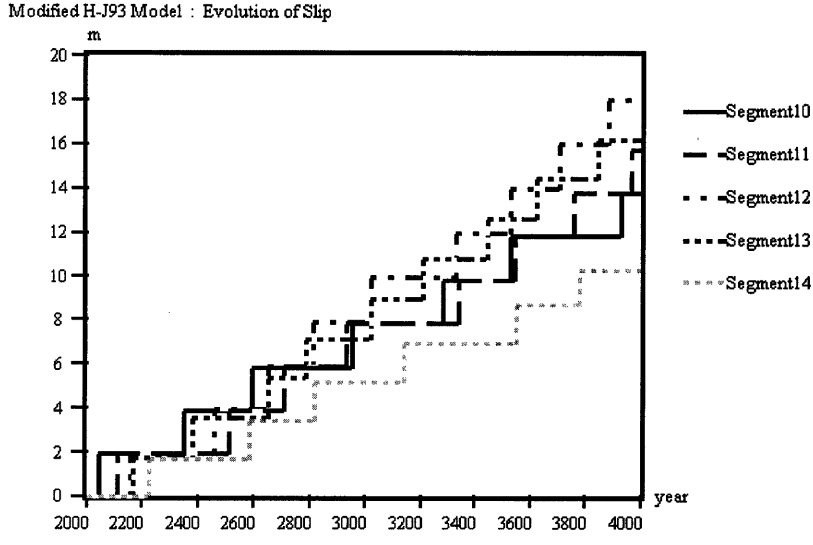

Fig. 6. Slip history of faults along (a) the Nankai trough and (b) the Median Tectonic Line during the period from 2000 to 4000.

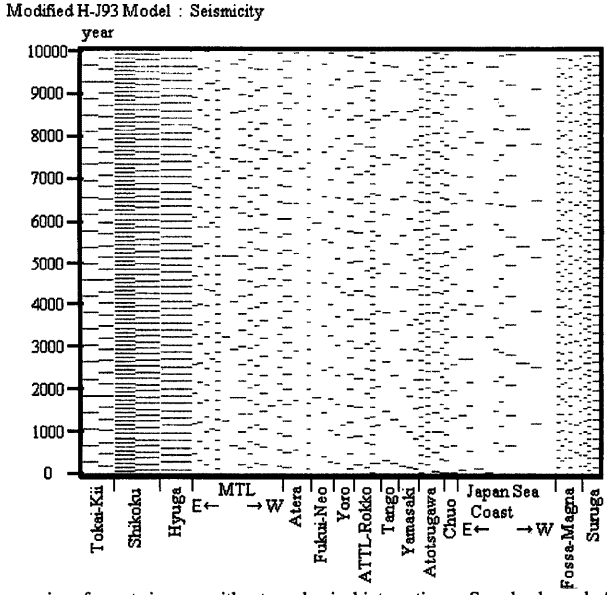

Fig. 7. Time series of events in case without mechanical interaction. See also legend of Fig. 3.

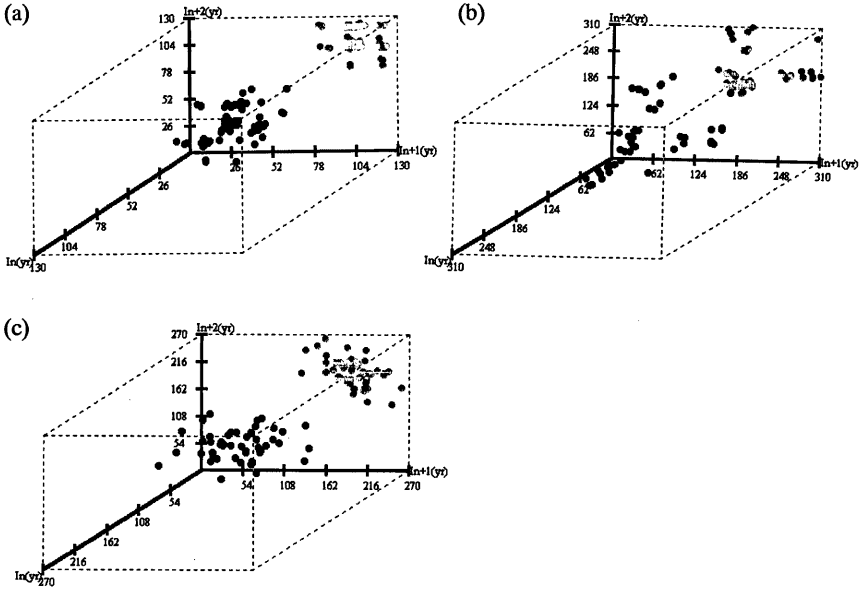

Fig. 8. Phase diagrams of attractor. Solid circles indicate a "state" whose component are recurrence intervals between four consecutive events, while grey ones are their projection onto a two-dimensional space. (a) Fault 2 off Shikoku along the Nankai trough. (b) Fault 12 in the Kii peninsula along the Median Tectonic Line. (c) Fault 30, the Rokko fault system.

Fig.6(a) and (b) shows accumulated slip against time for faults along the Nankai trough and MTL, respectively. Slip for events are almost constant for each fault: 4 ~ 6m for Nankai trough and ~ 2m for MTL. Because I specified stress as a threshold and size of faults are not the same, slips are not exactly equal to these value for all faults. Any of characteristic, time-predictable or slip-predictable model cannot be applied to activity during whole period (=10,000 years) for several fault. There are significantly longer intervals after three or four quasi-periodic cycles. Periodicity is disturbed by these longer intervals.

Fig.7 shows the simulated seismicity for the model without interaction. Each fault ruptures periodically. Activity as a whole system seems less than that with interaction.

3.2 Recurrence

Fig.4 is convenient to see the general figure of simulated seismicity, but characteristics of recurrence behavior of each fault are not clear. I prepare phase diagram similar to those by Rundle (1988a).

Fig.8 is phase diagram for 3 faults. In these diagrams, three components of plotted points are three intervals of four consecutive events and the set of these points is attractor. If events recur periodically, the attractor converges to a single point (Rundle, 1988a). It is clear that these three faults show complicated recurrence patterns and their behavior seems chaotic. Generally, interval becomes short after long rest, and vice versa, looking at the projection of attractor onto two dimensional plane. However, it is clear that there are two categories of recurrence behaviors. One is that intervals are distributed around the well defined average (Type I; Fig.8c). The other is that there are 2 or 3 separate intervals (Type II; Fig.8 a and b). There are a few faults that rupture periodically. For a few faults, events are not enough to examine recurrence behavior. Fig.9 show the classification of fault faults according to the type of recurrence behavior. Type II faults are distributed around the Kii peninsula. This is because large events recur quickly at the faults off Shikoku and its effect on surrounding faults are large enough to delay the next event at these faults to occur significantly. On the other hand, significant effects of events at inland faults are seen only on neighboring faults, especially near the edge, and its magnitude may be much smaller than stress release (Rundle, 1988a). Because I evaluate Δ CFF at the center of fault, effect may be smaller.

It is interesting that variation in recurrence interval from 50 % to 150 % for three faults. Several excavation studies suggest that recurrence intervals for inland faults in Japan varies in the range of 28 % to 184 % of its average (Kumamoto, 1998). This result suggests that fluctuation of recurrence interval might be caused by mechanical interaction, though the present model gives much shorter recurrence interval than the geologically obtained ones as mentioned above.

Fig. 10 is a phase diagram for the model without interaction. As mentioned above, attractor is a point in this case, which means events recur periodically.

3.3 Average Stress of the Whole System

It is interesting to examine the state of stress of the whole system. According to the idea of self-organized criticality, the system approaches to critical state spontaneously. Fig. 11 shows the temporal changes in averaged stresses for all faults with weight proportional to their area. With interaction, average stress drops largely every 1,000 years (Fig.11a). Before these events average stress rises. Therefore there seems to be a dominant rhythm in stress change. These large stress drops correspond to cascade events which rupture all faults along the Nankai trough. Without interaction, such a large stress drops are not recognized, but temporal change looks like white noise (Fig.11b). The above observation looks paradoxical, because behavior of specific fault is rather chaotic in the case with interaction. This means that long-term forecast of event at a specific fault is deterministically impossible, but large events which significantly drops stress level of the whole system can be forecast. However such a behavior cannot be seen if threshold of inland fault rises. This suggests that large contrast in stress drop of events gives rise such a behavior.

It is noteworthy that the average stress fluctuate around the about half of the limit level, which all fault is close to failure at the same time. This observation is also seen in the case with high threshold for inland faults. Two answer is possible. The first is that probability that average stress reaches the limit level may be very small, because all the fault must be close to failure and recurrence intervals of faults are different one another. Even in the case without interaction, average stress is half as large as the limit level, which may support this answer. The second is that interaction keeps away from rising stress level of the whole system, which is similar to the idea of self-organized criticality (Bak and Tang, 1989; Carlson and Langer, 1989; Ito and Matsuzaki, 1989). Even if several faults are approaching to failure level, one rupture event may cause another rupture and decline stress level. Since the number of trial is not so large, much more calculations are needed in order to resolve this problem.

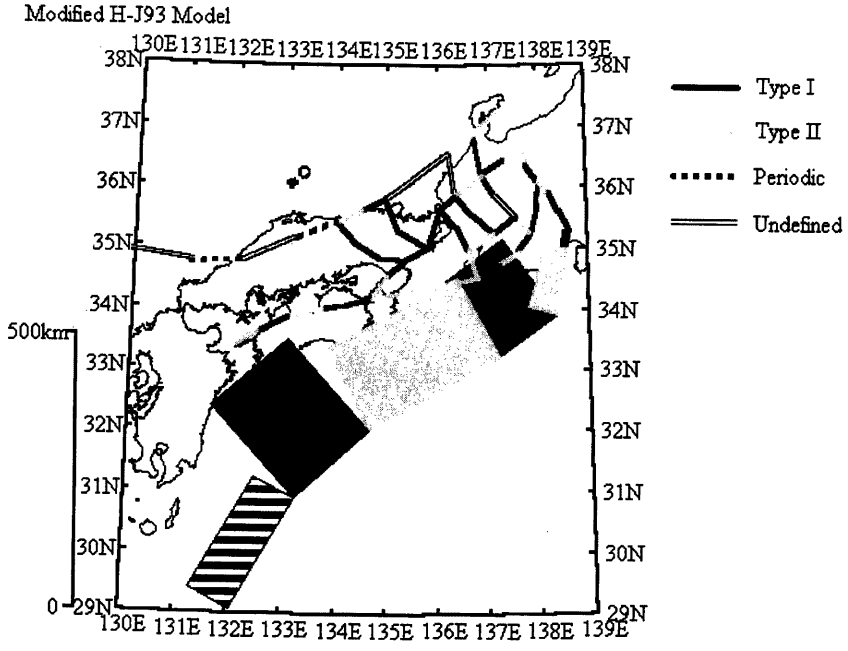

Fig. 9. Classification of faults according to characteristics of recurrence pattern.

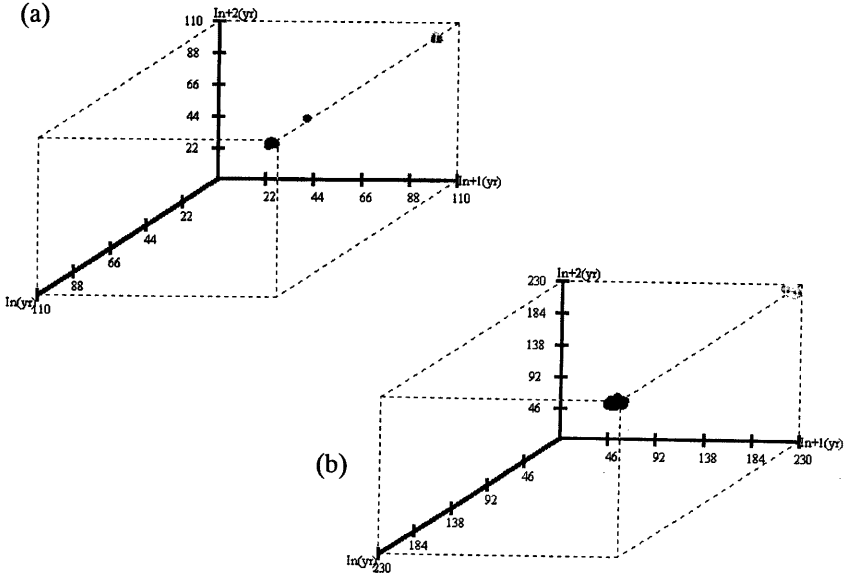

Fig. 10. Phase diagrams of attractors in case without interaction. (a) Fault 2. (b) Fault 30. See also legend of Fig. 8.

(a)

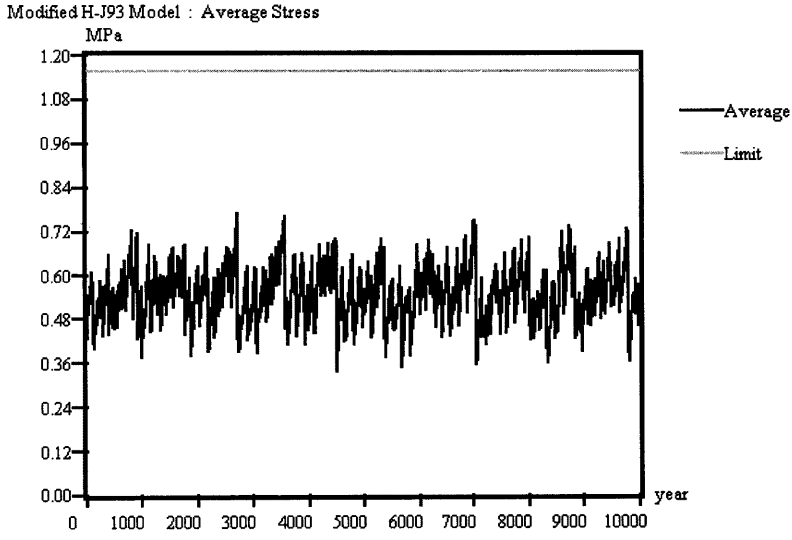

(b)

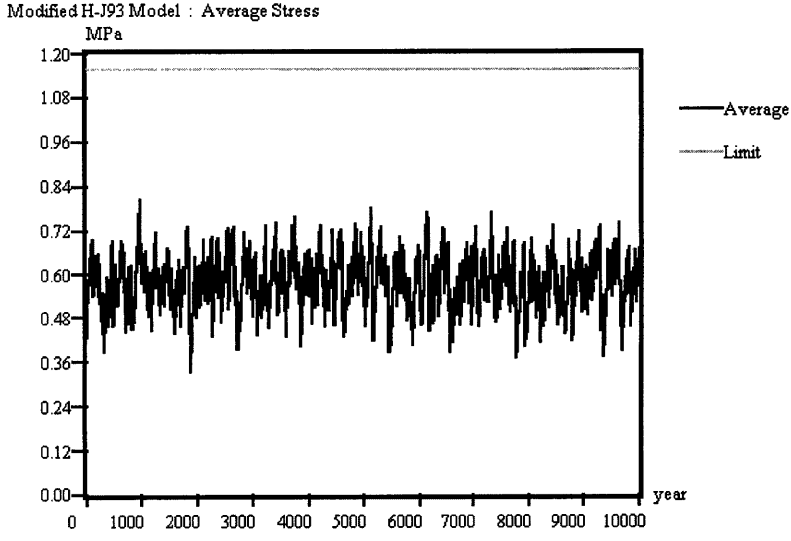

Fig. 11. Temporal variation in averaged stress weighted proportional to fault area. (a) Case with interaction. (b) Case without interaction.

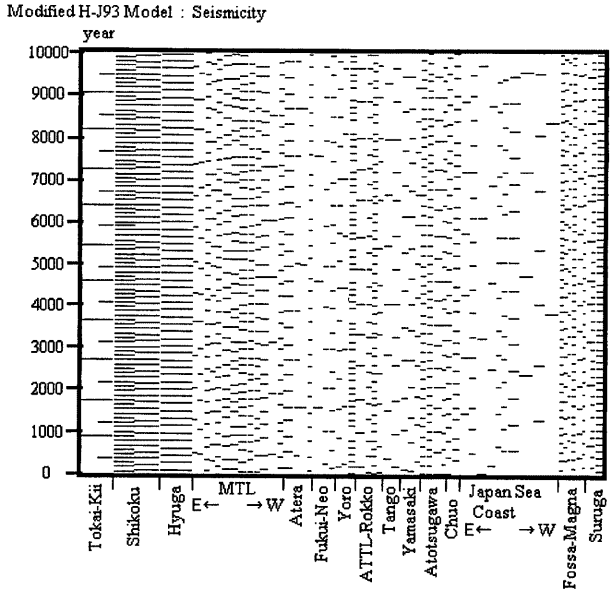

Fig. 12. Time series of events with 1% fluctuation in initial stresses

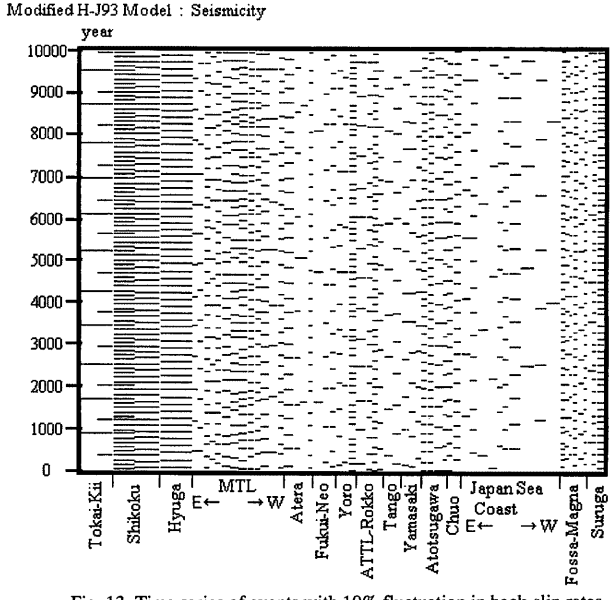

Fig. 13. Time series of events with 10% fluctuation in back-slip rates

3.4 Effects of Fluctuation of Initial State and Back-Slip Rate

In order to examine the error of some parameters in the model, I simulate seismicity in cases with fluctuation of initial stress and back-slip rate, respectively. For initial stress I assume only 1 % fluctuation. Fig. 12 shows the simulated seismicity for a case. During the first 1,000 years, there are no significant difference in simulated seismicity between Figs. 4 and 12. However rupture of several faults are delayed or advanced more than 100 years after that.

Estimate of back-slip rate is as large as 4 mm/yr in Hashimoto and Jackson's (1993) model. Considering this estimate, I adopt 10 % fluctuations for back-slip rate and simulate seismicity (Fig.13). In this case, difference can be seen before 500 years. After a couple of thousand years, the pattern is completely different between Figs. 4 and 13.

The above results cast a serious problem on long-term forecast of large events. In order to make an accurate forecast, we must observe stress and strains with less than a few percent. Therefore it is important to develop a probabilistic method to forecast large events.

4. Discussions

Results of simulation of seismicity taking mechanical interaction between faults into consideration suggest mechanical interaction may cause wide variety in behavior of faults. Rundle (1988a,b) and Ward (1996) already obtained similar results for southern California. This study confirms variety of recurrence behavior arises from mechanical interaction in convergence zones as well. It is interesting that there are two kinds of different pattern of recurrence in this study. This may be attributed to significant difference of slip rates and geometry between interplate and intraplate faults. It might be necessary to examine this point with a idealized model.

Activity of large events at MTL is much higher than that obtained from geological studies. In this model, however, slips must be too large if we want recurrence interval as long as 1,000 years. As mentioned above, this is because I use back-slip rates derived from geodetic data. These back-slip rates are estimated as dislocation in perfectly elastic medium. It is well known that geodetic strain rates are larger than geologic and seismological strain rates by a factor of 10 in the Japanese islands (Wesnousky et al., 1982; Iio, 1996; Ikeda, 1996). Iio (1996) pointed out that geodetic strain rates contain inelastic one and suggested that aseismic creep of inland faults at the depth of seismogenic zone may play an important role. The results of this simulation suggest that large part of geodetic strains are not accumulated as elastic strain but dissipated by such unknown inelastic processes as creep, plastic flow etc.

The present model assumes an elastic half space and as large rectangular faults with uniform slip as a source region of M7 or 8 earthquake. These assumption arises large stress concentration near the edge of faults, which may affect seismicity pattern even if stress is evaluated at the center of each fault. This model cannot produce smaller events than that characteristic to each fault. Furthermore forward-slip causes instantaneous and permanent changes in stress in the surrounding region, because of the assumption of perfect elasticity. Time delay of stress changes due to viscoelastic response of asthenosphere is not considered in this calculation. Therefore downsizing of modeled faults, effects of viscoelasticity of asthenosphere, fault consititutive relation, healing process etc. are to be considered in order to simulate more realistic recurrence intervals, statistical characteristics like Gutenburg – Richter law.

As discussed above, this study suggests that even a small fraction of errors in parameters cause large difference in patterns of resulted seismicity after hundreds of years. This may be a serious problem in the long-term forecast of earthquake occurrence. Even if simulator of crustal activity including above factors can be developed, estimate of parameters must be highly accurate. Furthermore the process is so highly nonlinear that the law of error propagation may not be applied. Therefore it is necessary to develop a method to estimate error in the forecast as well as to develop simulator itself.

5. Conclusions

Activity of large events in southwest Japan is simulated taking mechanical interaction into account and the following results are derived.

(1) Mechanical interaction arises a wide variety of recurrence behaviors of large events such as cascade, migration etc.

(2) Recurrence behavior is classified into two categories : recurrence interval of some faults fluctuates around well defined average, and the other faults have multiple discrete intervals. The second type faults are distributed around the Kii peninsula.

(3) Recurrence intervals of specific faults are within 50 ~ 150 % of its average.

(4) Small errors in initial stress and back-slip rates cause significant difference in simulated seismicity after hunderds of years, which cast a serious problem on long-term forecast of earthquake occurrence.

References

Bak, P., and Tang, C. (1989): Earthquakes as a self-organized critical phenomenon, *J. Geophys. Res.*, Vol.94, pp.15535-15537.

Burridge, R., and Knopoff, L. (1967): Model and theoretical seismicity, *Bull. Seismol. Soc. Amer.*, Vol.57, pp.341-371.

Carlson, J.M., and Langer, J.S. (1989): Mechanical model of an earthquake fault, *Phys. Rev.*, A40, pp.6470-6484.

Harris, R.A., and Simpson, R.W. (1992): Changes in static stress on southern California faults after the 1992 Landers earthquake, *Nature*, Vol.360, pp.251-254.

Hashimoto, M. (1995): Static stress changes associated with the Kobe earthquake : Calculation of changes in Coulomb failure function and comparison with seismicity change, *Zisin(J. Seismol. Soc. Jpn.), Ser. 2*, Vol. 48, pp.521-530 (in Japanese with English abstract).

Hashimoto, M. (1997): Correction to "Static stress changes associated with the Kobe earthquake : Calculation of changes in Coulomb failure function and comparison with seismicity change", *Zisin(J. Seismol. Soc. Jpn.), Ser. 2*, Vol. 50, pp.21-27 (in Japanese with English abstract).

Hashimoto, M. (1998): Simulation of temporal variation in Coulomb failure functions in the source region of the Hyogo-ken Nanbu earthquake, *Zisin(J. Seismol. Soc. Jpn.), Ser. 2*, Vol. 50, Supplement, pp.229-249 (in Japanese with English abstract).

Hashimoto, M. and Jackson, D.D. (1993): Plate tectonics and crustal deformation around the Japanese islands, *J. Geophys. Res.*, Vol.98, pp.16149-16166.

Hori, T. and Oike, K. (1996): A statistical model of temporal variation of seismicity in the Inner Zone of southwest Japan related to the great interplate earthquakes along the Nankai trough, *J. Phys. Earth*, Vol.44, pp.349-356.

Hori, T. and Oike, K. (1998): A physical mechanism for temporal variation in seismicity in the Inner Zone of southwest Japan related to the great interplate earthquakes along the Nankai trough, *submitted to Tectonophysics*.

Huang, J. and Turcotte, D.L. (1990): Evidence for chaotic fault interactions in the seismicity of the San Andreas fault and Nankai trough, *Nature*, Vol.348, pp.234-236.

Hudnut, K.W., Seeber, L. and Pacheco, J. (1989): Cross-fault triggering in the November 1987 Superstition Hills earthquake sequence, southern California, *Geophys. Res. Lett.*, Vol.16, pp.199-202.

Iio, Y. (1996): A possible generating process of the southern Hyogo Prefecture earthquake – Stick of fault and slip on detachment, *Zisin(J. Seismol. Soc. Jpn.), Ser. 2*, Vol.49, pp.103-112 (in Japanese with English abstract).

Ikeda, Y. (1996): Implications of active fault study for the present-day tectonics of the Japan arc, *Active Fault Research*, Vol.15, pp.93-96 (in Japanese with English abstract).

Ito, K. and Matsuzaki, M. (1989): Earthquake as self-organized critical phenomena, *J. Geophys. Res.*, Vol.95, pp.6853-6860.

Jaume, S.C. and Sykes, L.R. (1992): Changes in state of stress on the southern San Andreas fault resulting from the California earthquake sequencee of April to June 1992, *Science*, Vol.258, pp.1325-1328.

King, G.C.P., Stein, R. and Lin, J. (1994): Static stress changes and the triggering of earthquakes, *Bull. Seismol. Soc. Amer.*, Vol.84, pp.935-953.

Kumamoto, T. (1998): Long-term conditional seismic hazard of Quaternay active fautls in Japan, *Zisin(J. Seismol. Soc. Jpn.), Ser. 2*, Vol.50, Suppl., pp.53-71 (in Japanese with English abstract).

Matsu'ura, M., Jackson, D.D. and Cheng, A.B. (1986): Dislocation model for aseismic crustal deformation at Hollister, California, *J. Geophys. Res.*, Vol.91, pp.12661-12674.

Okada, Y. (1992): Internal deformation due to shear and tensile faults in a half-space, *Bull. Seismol. Soc. Amer.*, Vol.82, pp.1018-1040.

Pollitz, F.F. and Sacks, I.S. (1997): The 1995 Kobe, Japan, earthquake: A long-delayed aftershock of the offshore 1944 Tonankai and 1946 Nankaido earthquake, *Bull. Seismol. Soc. Amer.*, Vol.87, pp.1-10

Ruff, L.J. (1992): Asperity distributions and large earthquake occurrence in subduction zones, *Tectonophysics*, Vol.211, pp.61-83.

Rundle, J.B. (1988a), A physical model for earthquakes 1. Fluctuations and interactions, *J. Geophys. Res.*, Vol.93, pp.6237-6254.

Rundle, J.B. (1988b): A physical model for earthquake 2. Application to southern California, *J. Geophys. Res.*, Vol.93, pp.6255-6274.

Rundle, J.B. and Kanamori, H. (1987): Application of an inhomogeneous stress (patch) model to complex subduction zone earthquakes : A discrete interaction matrix approach, *J. Geophys. Res.*, Vol. 92, pp.2606-2616.

Savage, J.C. (1982): A dislocation model of strain accumulation and release at a subduction zone, *J. Geophys. Res.*, Vol.88, pp.4984-4996.

Schwarz, D.P. and Coppersmith, K.J. (1984): Fault behavior and characteristic earthquakes: examples from the Wasatch and San Andreas faults zones, *J. Geophys. Res.*, Vol.89, pp.5581-5598.

Tsutsumi, H. and Okada, A. (1995): Faultation and Holocene surface faulting on the Median Tectonic Line, southwest Japan, *J. Geophys. Res.*, Vol.101, pp.5855-5871.

Ward, S.N. (1996): A sythetic seismicity model for

southern California,: Cycles, probabilities, and hazards, *J. Geopys. Res.*, Vol.101, pp.22393-22418.

Wesnousky, S.G., Scholz, C.H. and Shimazaki, K. (1982): Deformation of an island arc: rates of moment release and crustal shortening in intraplate Japan determined from seismicity and Quaternary fault data, *J. Geophys. Res.*, Vol.87, pp.6829-6852.

要　旨

西南日本の大地震の活動をプレート間及びプレート内地震の間の力学的な相互作用を考慮したモデルによりシミュレートすることを試みた．このモデルでは，それぞれの断層で測地データのインバージョンにより推定されたバック･スリップに応じて応力が蓄積し，それがしきい値を越えると地震が起き，応力が再配分される．

シミュレーションの結果，相互作用によりカスケードや移動現象などの複雑なパターンが生じることが明らかになった．断層によって，繰り返し間隔がある平均の周りにばらつくものと，２～３の繰り返し間隔を持つものに分かれ，後者は紀伊半島の周辺に多いことが示された．また，初期値の小さな誤差により数百年後の地震活動に大きな差が生じることも示された．

キーワード: 地震活動シミュレーション；断層間相互作用；クーロン破壊関数；地震の再来間隔；バック・スリップ・モデル